Advances in Applied Mathematics and Mechanics
Adv. Appl. Math. Mech., Vol. **11**, No. 1, pp. 1-19

DOI: 10.4208/aamm.OA-2018-0188
October 2019

A Reduced Basis Method for the Nonlinear Poisson-Boltzmann Equation

Lijie Ji[1], Yanlai Chen[2,*] and Zhenli Xu[3]

[1] *School of Mathematical Sciences, Shanghai Jiao Tong University, Shanghai 200240, China*
[2] *Department of Mathematics, University of Massachusetts Dartmouth, 285 Old Westport Road, North Dartmouth, MA 02747, USA*
[3] *School of Mathematical Sciences, Institute of Natural Sciences and Key Laboratory of Scientific and Engineering Computing (Ministry of Education), Shanghai Jiao Tong University, Shanghai 200240, China*

Received 29 August 2018; Accepted (in revised version) 8 January 2019

Abstract. In numerical simulations of many charged systems at the micro/nano scale, a common theme is the repeated resolution of the Poisson-Boltzmann equation. This task proves challenging, if not entirely infeasible, largely due to the nonlinearity of the equation and the high dimensionality of the physical and parametric domains with the latter emulating the system configuration. In this paper, we for the first time adapt a mathematically rigorous and computationally efficient model order reduction paradigm, the so-called reduced basis method (RBM), to mitigate this challenge. We adopt a finite difference method as the mandatory underlying scheme to produce the high-fidelity numerical solutions of the Poisson-Boltzmann equation upon which the fast RBM algorithm is built and its performance is measured against. Numerical tests presented in this paper demonstrate the high efficiency and accuracy of the fast algorithm, the reliability of its error estimation, as well as its capability in effectively capturing the boundary layer.

AMS subject classifications: 65M10, 78A48
Key words: Reduced order modeling, reduced basis method, Poisson-Boltzmann equation, differential capacitance.

1 Introduction

Fast numerical algorithms for solving parametrized partial differential equations (PDEs) have attracted wide-spread interest in recent years, particularly in engineering applications due to many control, optimization and design problems requiring repeated simulation of certain parametrized PDEs. Traditional numerical methods solve the equation

*Corresponding author.
Emails: sjtujidreamer@sjtu.edu.cn (L. J. Ji), yanlai.chen@umassd.edu (Y. L. Chen), xuzl@sjtu.edu.cn (Z. L. Xu)

for each necessary parameter value and thus obtaining the solution ensemble for the whole parameter space is potentially time-consuming if not entirely infeasible. This is an especially onerous task if the physical and/or parametric domain are of high dimensions. It is therefore imperative to design efficient and accurate reduced order modeling techniques for these scenarios capable of realizing negligible marginal (i.e., per parameter value) computational cost. The reduced basis method (RBM) provides a rigorous and highly efficient platform to achieve this exact goal. It was first introduced for nonlinear structure problem [1, 35] in 1970s and has been later analyzed and extended to solve many problems such as linear evolutionary equation [21], viscous Burgers equation [41], Navier-Stokes equations [14] and harmonic Maxwell's equation [10,11] just to name a few. Interested readers are referred to the review papers [19,37] and recent monographs [22,36] for a systematic description of the RBM.

One such parametric scenario we are concerned in this paper is the simulation of the electrostatic interaction which is essential for many systems in physical, biological and materials sciences [16, 30, 42] at the nano/micro scale. These include, for example, biopolymers, colloidal suspensions and electrochemical energy devices. The Poisson-Boltzmann (PB) theory [3,7,15,17] plays a fundamental role in understanding the electrostatic phenomenon in such systems. It subjects the electric potential of a charged system at the equilibrium state to a nonlinear elliptic equation with the the Boltzmann distribution for the ionic densities. The numerical solution of the PB equation has been widely studied in literature [2, 34] and the numerical solvers are implemented in many popular software packages such as Delphi and APBS for practical simulations. However, one often needs to solve the PB equation repeatedly to determine certain physical quantities of interest (QoI) which are usually dependent on a wide range of parameters delineating e.g., the boundary voltage, the geometric length and the Debye length. Particular examples of such QoIs include the electrochemical capacitance, the current-voltage relation and the free-energy calculation etc.

In this work, we propose a reduced basis method for the parametrized nonlinear PB equation. Model order reduction for nonlinear equations is often realized by linearization techniques [44] or polynomial approximations, among others. One frequently-used tool is the empirical interpolation method (EIM) [5,18] which is crucial to facilitate the offline-online decomposition, a hallmark feature of RBM to realize the negligible marginal computational cost. This paper extends the RBM for the nonlinear PB equation by approximating the nonlinear exponential term with a Taylor expansion form [39]. This leads to a linear equation in each calculation step. Realizing a partial offline-online decomposition, the method promises high accuracy due to the avoidance of the EIM error. It is noted that this work only focuses on the mean-field PB equation which is limited to describe phenomena when many-body interactions are important. The extension of our work to the modified PB equations such as those including correlation and steric effects (see, e.g., [32] and references therein) is of great interest due to the complex electrostatic phenomena they model and the drastically different nonlinearity contained therein. The successful application of the RBM will be reported in the future. We also note that Kweyu

et al. [28,29] has recently extended the RBM to the linearized PB equation for electrostatic solvation calculations of the biomolecules. To the best of our knowledge, this paper is the first attempt of solving the fully nonlinear equation with rapid nonlinearity by the RBM.

The paper is organized as follows. In Section 2, we introduce the basic RB algorithm. Detailed description of the PB model, the FDM scheme used to obtain our high-fidelity approximation, how we apply RB to the nonlinear PB equation and its computational analysis are provided in Section 3. In Section 4, we show numerical results in both one and two physical dimensional spaces to demonstrate the accuracy and efficiency of our reduced model. Finally, concluding remarks are drawn in Section 5.

2 Overview of the reduced basis method

The reduced basis method is a fast algorithm for computing a certified surrogate to the highly accurate but potentially expensive numerical solution (termed high-fidelity truth approximation in this context) of a system dependent on a P-dimensional parameter

$$\mu \in \mathcal{D} \subset \mathbb{R}^P.$$

It is particularly useful for the many-query or real-time simulation context where an initial investment may pay off through repeated simulations with significantly less (at times negligible) marginal cost at a later stage. An essential tool is the offline-online decomposition process. The offline phase is devoted to construct the RB space, denoted by W_N (with N being its dimension and usually much smaller than the number of degrees of freedom for the high-fidelity truth approximation). During the online stage, an RB approximation for any given parameter value μ in the prescribed domain $\mathcal{D}$ is sought from the space W_N. We remark that the RB approximations do not necessarily have low-fidelity. In fact, they often match the accuracy of the high-fidelity approximation with a rather small N.

Since the online solver (of various dimensions) is invoked repeatedly offline to construct the RB space W_N through a greedy algorithm, we present here the crucial online solver for a linear PDE and postpone the construction of the RB space until when we describe the RBM for the nonlinear PB equation for completeness of that section. Indeed, consider a linear elliptic PDE, $L(\mu)u(x,y) = f(x,y)$, with the operator (and/or the right hand side) parametrized by μ. Let $\mathcal{N}$ be the number of degrees of freedom for a well-defined and accurate numerical scheme (termed truth solver in the RB context) discretizing this equation. The numerical approximation $u^{\mathcal{N}}(\mu)$ is the solution of

$$L_{\mathcal{N}}(\mu)u^{\mathcal{N}} = f, \tag{2.1}$$

which can be understood as deriving from a collocation formulation, $L_{\mathcal{N}}(\mu)u^{\mathcal{N}}(x,y) = f(x,y)$ for certain (x,y)'s, or a Galerkin scheme, $a^{\mathcal{N}}(u^{\mathcal{N}},v) = f(v)$ for $\forall v$. A critical assumption for the operator $L_{\mathcal{N}}$ is that it is affine with respect to (the functions of) the

parameter. That is, it can be written as,

$$L_{\mathcal{N}} = \sum_{q=1}^{Q} B_q(\mu) L_{\mathcal{N}}^q, \tag{2.2}$$

where $L_{\mathcal{N}}^q$ is a parameter-independent operator and coefficient function B_q depends on parameter μ. We note that, when the condition (2.2) is violated (e.g., the parameter dependence is not affine or the equation is nonlinear, that is, (2.1) becomes $L_{\mathcal{N}}(u^{\mathcal{N}};\mu) = f$), special care needs to be taken to facilitate the design of RBM. Indeed, EIM [5,18] will be applied to recover the affine dependence and/or linearization techniques will be in place to transform the nonlinear solves into a sequence of linear solves. The RBM is built upon this discrete solution and its accuracy is also measured against it, as opposed to the exact solution of the equation $L(\mu)u(x,y) = f(x,y)$. For that reason, the solution of Eq. (2.1) is considered "exact" from the perspective of RBM and thus called the high-fidelity truth approximation. For simplicity of exposition, we shall drop the superscript $\mathcal{N}$ in the remainder of the paper as we will not make any reference to the exact solution of the PDE.

The online process of the RBM is as follows. Assuming that we have identified N parameter values $\{\mu^1,\cdots,\mu^N\}$ and the corresponding high-fidelity truth approximations $u_n \equiv u^{\mathcal{N}}(\mu^n)$, $1 \le n \le N$. With a slight abuse of notation, we do not differentiate these functions and their discrete vectors. These vectors constitute the basis space of the RBM, written in the form of a matrix, $W_N = [u_1,\cdots,u_N] \in \mathbb{R}^{\mathcal{N}\times N}$. One expresses the RB approximation as a linear combination of the basis vectors. That is, we have

$$\widehat{u}(\mu) = W_N c(\mu), \tag{2.3}$$

where $c(\mu) \in \mathbb{R}^N$ is the RB coefficient vector. These coefficients are sought by satisfying the ansatz of the PDE. Therefore, we substitute this combination into Eq. (2.1) to obtain a linear algebra system,

$$A(\mu)c(\mu) = f, \tag{2.4}$$

where $A(\mu) = L_{\mathcal{N}} W_N$ is a $\mathcal{N}\times N$ matrix, $f \in \mathbb{R}^{\mathcal{N}}$ is a column vector and $\mathcal{N} \gg N$.

Coefficients $c(\mu)$ can be obtained by the least-squares method leading to a Petrov-Galerkin approach. One can also resort to the following Galerkin approach to identify $c(\mu)$ as a solution of the following (reduced) linear system:

$$B(\mu)c(\mu) = f_N. \tag{2.5}$$

Here $B(\mu)$ is the RB matrix of dimension $N\times N$ and f_N is the RB vector of dimension N, which are expressed as follows,

$$B(\mu) = W_N^T L_{\mathcal{N}}(\mu) W_N, \qquad f_N(\mu) = W_N^T f. \tag{2.6}$$

Obviously, this is an energy projection into the RB space $\text{span}\{u_n : 1 \le n \le N\}$. Solving equation (2.5) is much cheaper than solving Eq. (2.1) and system (2.5) is an order reduction in comparison to system (2.1).

3 Poisson-Boltzmann equation and its reduced model

3.1 Poisson-Boltzmann model and the high-fidelity approximation

Poisson-Boltzmann is a mean-field theory describing the equilibrium distribution of charged systems [13,27,31,43], which has been widely used in biomolecular solvation, microfluidic devices and charged soft materials. Typically, one considers a symmetric binary electrolyte between two parallel electrodes positioned at locations marked by $X=\pm L_X$ with the extremes of the other direction marked $Y=\pm L_Y$. The PB equation for the electric potential ϕ is written as,

$$\nabla\cdot(\varepsilon\nabla\phi)=2zec_0\sinh(\beta ze\phi)-\rho_f, \tag{3.1}$$

where ε is the dielectric permittivity, $\pm ze$ is the charge of an cation or anion, β is the inverse thermal energy, c_0 is the bulk concentration and ρ_f is the density of the fixed charge.

Without loss of generality, we let the computational domain be a 2D square by setting $L_X=L_Y=L$. We further set $x=X/L$, $y=Y/L$, $\varepsilon=\varepsilon_W$ being a constant, $\Phi=ze\beta\phi$ and $g=\rho_f/(2zec_0)$. Then Eq. (3.1) becomes the following dimensionless PB equation,

$$D\nabla^2\Phi=\sinh\Phi+g(x,y), \tag{3.2}$$

where $D=(\ell_D/L)^2$, $\ell_D=1/\sqrt{8\pi\ell_B z^2 c_0}$ is the Debye screening length and $\ell_B=\beta e^2/(4\pi\varepsilon_W)$ is the Bjerrum length in water solvent. The Laplace operator ∇^2 is with respect to the new coordinates (x,y) and the computational domain in (x,y) is now $\Omega=[-1,1]^2$. We introduce the following boundary conditions,

$$\Phi(x=\pm1,y)=\pm V, \tag{3.3a}$$

$$\partial_y\Phi(x,y=\pm1)=0. \tag{3.3b}$$

Here, the first boundary condition represents the fixed boundary voltages on the left and right electrodes and the second one characterizes a state of low dielectric permittivity at top and bottom boundaries $y=\pm1$. Eq. (3.2) is thus the PB equation parametrized by

$$\mu:=[D,V],$$

a vector-valued parameter. We intend to devise a RBM for its rapid resolution for scenarios when it needs to be solved repeatedly for a wide range of μ values. More parameters may be considered resulting in a higher-dimensional μ. The offline phase will then potentially suffer from the curse of dimensionality, prompting the active research area of offline enhancement for RBM. Existing approaches toward this end include multistage greedy algorithm [38], training set adaptivity and adaptive parameter domain partitioning [20], random greedy sampling [23], greedy sampling acceleration through nonlinear optimization [40] and multi-level greedy algorithm based on adaptive construction of surrogate training sets [26].

3.1.1 The iterative truth solver

Before the discussion of the RBM, let us describe a finite-difference solver for the nonlinear PB equation. Numerical methods for nonlinear PB equations have been widely studied [4,6,8,33,34]. In this paper, we use the similar technique as Shestakov et al. [39], which solves the nonlinear equation by iteratively transforming it into a linear one through truncating the Taylor series. Let Φ_m be the approximate solution at the mth iterative step, then for the solution at the $(m+1)$th step, the nonlinear term $\sinh\Phi_{m+1}$ is approximated by,

$$\sinh\Phi_{m+1}\approx\sinh\Phi_m+(\cosh\Phi_m)(\Phi_{m+1}-\Phi_m) \tag{3.4}$$

and the PB equation then becomes,

$$-D\nabla^2\Phi_{m+1}+(\cosh\Phi_m)\Phi_{m+1}=(\cosh\Phi_m)\Phi_m-\sinh\Phi_m-g(x,y). \tag{3.5}$$

We then use the second-order five-point central difference scheme to approximate $\nabla^2\Phi$, leading to a linear system for Φ_{m+1}. To describe this system, we denote by $\mathcal{N}$ the total number of grid points discretizing the physical domain. The number of free nodes, i.e., those in the interior of the domain and on boundaries $y=\pm1$ is denoted by $\mathcal{N}_0$. This means that there are $\mathcal{N}-\mathcal{N}_0$ nodes on boundaries $x=\pm1$ for which the corresponding potential values are specified. Let $\mathcal{L}_{\mathcal{N}}(\mu;\Phi)$ be the discretized operator for approximating the left hand side of Eq. (3.5) and Neumann boundary condition (3.3b). Let $\vec{\Phi}$ be the $(\mathcal{N}_0\times1)$ vector representing the discretized function $\Phi(x,y)$. The numerical scheme can then be written as

$$\mathcal{L}_{\mathcal{N}}(\mu;\Phi_m)\vec{\Phi}_{m+1}=\vec{F}(\Phi_m), \tag{3.6}$$

for $m=0,1,\cdots$. Here $\vec{F}$ discretizes the right hand side of equation (3.5) and incorporates the Dirichlet boundary condition (3.3a). The iterative algorithm for solving (3.2) is summarized in Algorithm 1 and the resulting solution $\Phi(\mu)$ is called the high-fidelity truth approximation corresponding to parameter μ in the RBM framework. Note that Eq. (3.6), being linear, is in fact only a tool for solving the noninear equation (3.2). Indeed, each resolution of (3.2) for a given μ amounts to a sequence of solves of (3.6). In other words, we are solving the full nonlinear PB equation, not a linearized one. The RB scheme is then built for the nonlinear PB equation.

Algorithm 1 Iterative solver for the nonlinear PB equation (3.2).

1: Initialize potential distribution Φ_0, $m=0$ and the tolerance $\delta_0=1$.
2: **while** $\delta_m>10^{-11}$ **do**
3: Solving the linear system of equations (3.6);
4: Set $\delta_{m+1}=||\vec{\Phi}_{m+1}-\vec{\Phi}_m||_\infty$;
5: Set $m=m+1$;
6: $\Phi(\mu)=\Phi_m$.

3.1.2 The quantity of interest

For most parametric systems, there are frequently quantities of interest which are nothing but functions of the parameter(s) describing the system. These QoIs are often calculated as functionals of the field variable, i.e., solution of the PDE modeling the system. Therefore, the efficient resolution of these field variables immediately leads to that of the QoI.

The electrochemical systems [12] of interest in this paper are no exceptions. Indeed, we are concerned with the total differential capacitance of the symmetric electrolyte. It is defined as $C=C_L/2$, where C_L is the differential capacitance of the left electrode defined by

$$C_L=\frac{d\sigma(V)}{dV} \quad \text{with } \sigma(V)=D\frac{\partial\overline{\Phi}}{\partial x}(x=-1),$$

where $\sigma(V)$ is the *surface charge density* at the left electrode. $\overline{\Phi}(x)$ is the average electric potential which is simply $\Phi(x)$ if the physical domain is one-dimensional and, for 2D, is nothing but

$$\overline{\Phi}(x)=\int_{-1}^{1}\Phi(x,y)dy.$$

For the one-dimensional case, one can derive an explicit expression for the differential capacitance C_L by solving the PB equation. Indeed, integrating Eq. (3.2) from x to 0 gives

$$\frac{d\Phi}{dx}=-\frac{2}{\sqrt{D}}\sinh\left(\frac{\Phi}{2}\right), \tag{3.7}$$

then one has, by utilizing the boundary condition, that $\sigma=-2\sqrt{D}\sinh(-V/2)$, which means,

$$C_L=-\frac{d\sigma}{dV}=\sqrt{D}\cosh\left(\frac{V}{2}\right). \tag{3.8}$$

3.2 Reduced basis method for the Poisson-Boltzmann equation

As shown in the overview, the online procedure of the RBM algorithm is to find the coefficients of the surrogate solution in the reduced basis space. Indeed, the N dimensional coefficient vector $c(\mu)$ is sought by asking the resulting surrogate solution to satisfy the PDE (3.6) weakly in the RB space,

$$A(\mu;\widehat{\Phi}_m)c_{m+1}(\mu)=W_N^T\vec{F}(\widehat{\Phi}_m),\quad m=0,1,\cdots, \tag{3.9}$$

at every iteration. Here, $c_{m+1}(\mu)$ denotes the $m+1^{\text{th}}$ iterate of the RB coefficient vector $c(\mu)$ and $\widehat{\Phi}_m$ is the m^{th} iterate of the RB solution,

$$\widehat{\Phi}_m(\mu)=W_Nc_m(\mu). \tag{3.10}$$

Note that $A(\mu;\widehat{\Phi}_m)=W_N^T\mathcal{L}_{\mathcal{N}}(\mu;\widehat{\Phi}_m)W_N$ depends on the current iterate of the RB solution $\widehat{\Phi}_m(\mu)$.

Thus, we have to rely on an online (reduced) iterative solver as well. This iterative procedure for solving the coefficient $c(\mu)$ is summarized in Algorithm 2 for any given parameter μ with the final RB surrogate approximation denoted by $c(\mu)$.

Algorithm 2 RB approximation for nonlinear PB equation, $c(\mu)$=RBM_PB(W_N,μ).

1: Initialize the potential distribution Φ_0, $j=0$, and the tolerance $\delta_0=1$.
2: **while** $\delta_j>10^{-8}$ **do**
3: Form the coefficient matrix A and $W_N^T\vec{F}$ at each jth iteration.
4: Solve for c_{j+1} from (3.9).
5: $\Phi_{j+1}=W_N c_{j+1}$.
6: $\delta_{j+1}=||\Phi_j-\Phi_{j+1}||_\infty$
7: j = j+1
8: $c(\mu)=c_j$.

The full offline algorithm for constructing RB basis space W_N is realized with standard greedy algorithm [22,36,37], which exploits a rigorous (albeit costly) *a posteriori* error estimator. We first discretize the parameter domain $\mathcal{D}$ by a sufficiently fine training set Ξ_{train}. We remark that a priori information, if available, can be leveraged for this discretization. For example, if μ follows certain probability distribution, Ξ_{train} could be obtained by sampling the parameter domain $\mathcal{D}$ according to the probability density function. The RBM algorithm is independent of how Ξ_{train} is obtained. The greedy algorithm then starts by selecting the first parameter μ^1 randomly from Ξ_{train} and obtaining its corresponding *high-fidelity truth approximation* $\Phi(\mu^1)$ from Algorithm 1 to form a (one-dimensional) RB space $W_1=\{\Phi(\mu^1)\}$. Next, we solve Eq. (3.9) to obtain an RB approximation $\widehat{\Phi}(\mu)$ for each parameter in Ξ_{train} together with an error bound $\Delta_1(\mu)$. The greedy choice for the $(i+1)$th parameter ($i=1,\cdots,N-1$) is made by

$$\mu^{i+1}=\arg\max_{\mu\in\Xi_{\text{train}}}\Delta_i(\mu). \tag{3.11}$$

The error bound is traditionally residual-based (i.e., $(F-\mathcal{L}_{\mathcal{N}}(\mu)\widehat{\Phi}(\mu))$-based) [22,36,37],

$$\Delta_i(\mu)=\frac{||F-\mathcal{L}_{\mathcal{N}}(\mu)\widehat{\Phi}(\mu)||_2}{\sqrt{\beta_{LB}(\mu)}}, \tag{3.12}$$

where $\beta_{LB}(\mu)$ is the smallest eigenvalue of $\mathcal{L}_{\mathcal{N}}(\mu)^T\mathcal{L}_{\mathcal{N}}(\mu)$. For simplicity, we compute it from the linear part of the operator (3.5). This stability constant is usually calculated by the Successive Constraint Method (SCM) [9,24,25] which is not necessary as the parameter dependence of the eigenvalue is obvious. After obtaining the $(i+1)$th high-fidelity truth approximation $\Phi(\mu^{i+1})$ from Algorithm 1, we augment the RB space by $W_{i+1}=\text{GS}(W_i,\vec{\Phi}(\mu^{i+1}))$, where $\text{GS}(W_i,\vec{\Phi}(\mu^{i+1}))$ denotes a Gram-Schmidt orthogonalization procedure of the new vector $\vec{\Phi}(\mu^{i+1})$ with respect to the previously selected and

Algorithm 3 Reduced basis greedy sampling algorithm.

0. Choose μ^1 randomly in Ξ_{train} and solve $\Phi(\mu^1)$ from Algorithm 1
1. Initialize $W_1=\{\Phi(\mu^1)\}$,
2. **For** $N=2,\ldots,N_{\max}$
3. Solve$c(\mu)$ from Algorithm. 2 and calculate $\Delta_{N-1}(\mu)$ for all $\mu\in\Xi_{\text{train}}$
4. Find$\mu^N=\arg\max_{\mu\in\Xi_{\text{train}}}\Delta_{N-1}(\mu)$
5. Solve$\Phi(\mu^N)$ from Algorithm 1 and orthogonalize$W_N=\text{GS}(W_{N-1},\Phi(\mu^N))$.
6. **End For**

orthogonalized basis vectors in W_i. The detailed numerical scheme is described in Algorithm 3.

With the greedy sampling algorithm, we still have to form and solve, in each iteration, the smaller RB systems in Step 3 for all μ in the training set. While solving the RB system is inexpensive, forming it can be much more expensive. However, for a particular set of parametrized linear systems, the RB system can be formed efficiently. The technique is an offline-online decomposition which is the topic of the next subsection.

3.2.1 Offline-online computational procedure

To describe this procedure, we revisit the original FDM scheme (3.6) for the nonlinear PB equation. $\mathcal{L}_{\mathcal{N}}(\mu)$ and $\vec{F}(\mu)$ are the discretized operator and the right hand side vector. For the purpose of forming the RB operator $A(\mu)$ in Eq. (3.9) efficiently, we decompose $\mathcal{L}_{\mathcal{N}}(\mu)$ at each mth iteration as follows

$$\mathcal{L}_{\mathcal{N}}(\mu;\Phi_m)=D\mathcal{L}^1_{\mathcal{N}}+\mathcal{L}^2_{\mathcal{N}}(\mu;\Phi_m). \tag{3.13}$$

Here, $D\mathcal{L}^1_{\mathcal{N}}$ is the first part ($-D\nabla^2$) of Eq. (3.5) having an explicit μ-dependence (note $\mu=(D,V)$) but is Φ_m-independent

$$\begin{aligned}\left(\mathcal{L}^1_{\mathcal{N}}\Phi_{m+1}\right)(x_j,y_k)=&-\frac{\Phi_{m+1}(x_{j-1},y_k)-2\Phi_{m+1}(x_j,y_k)+\Phi_{m+1}(x_{j+1},y_k)}{h_x^2}\\&-\frac{\Phi_{m+1}(x_j,y_{k-1})-2\Phi_{m+1}(x_j,y_k)+\Phi_{m+1}(x_j,y_{k+1})}{h_y^2},\end{aligned} \tag{3.14}$$

while $\mathcal{L}^2_{\mathcal{N}}(\mu;\Phi_m)$ denotes the second part of Eq. (3.5) that depends on both μ and Φ_m. When applied to Φ_{m+1}, it produces

$$\left(\mathcal{L}^2_{\mathcal{N}}(\mu;\Phi_m)\Phi_{m+1}\right)(x_j,y_k)=\cosh(\Phi_m(x_j,y_k))\Phi_{m+1}(x_j,y_k).$$

Here $h_x=2/N_x$, $h_y=2/N_y$, with N_x and N_y being the number of intervals in x-direction and y-direction, respectively. After this decomposition, $A(\mu;\widehat{\Phi}_m)$ can be written as

$$A(\mu;\widehat{\Phi}_m)=W_N^T\mathcal{L}_{\mathcal{N}}(\mu;\widehat{\Phi}_m)W_N=A_1(\mu)+A_2(\mu;\widehat{\Phi}_m), \tag{3.15}$$

where

$$A_1(\mu)=DW_N^T\mathcal{L}_{\mathcal{N}}^1W_N,$$
$$A_2(\mu;\widehat{\Phi}_m)=W_N^T\mathcal{L}_{\mathcal{N}}^2(\mu;\widehat{\Phi}_m)W_N.$$

Below is a summary of the decomposition and the operation count that each step takes.

- Realizing $W_N^T\mathcal{L}_{\mathcal{N}}^1W_N$ is μ-independent, we precompute it by gradually populating this $N\times N$ matrix as we identify the RB bases in the space W_N one by one. Indeed, when the ith basis is determined, we populate the ith row and ith column of $W_N^T\mathcal{L}_{\mathcal{N}}^1W_N$. This step takes $\mathcal{O}(N^2)$ operations.
- Update $A_2(\mu;\widehat{\Phi}_m)$ and the right hand vector $W_N^T\vec{F}(\widehat{\Phi}_m)$ at each iteration of the online procedure. This step takes $\mathcal{O}(\mathcal{N}_0N)$ operations.
- Invert the RB matrix $A(\mu)$ with $\mathcal{O}(N^3)$ operations.
- Form $\widehat{\Phi}(\mu)=W_Nc(\mu)$ after each iteration, taking $\mathcal{O}(\mathcal{N}_0N)$ operations.

Therefore, the total operation count of the online stage is

$$\mathcal{O}(\mathcal{N}_0N+N^3).$$

Although having $\mathcal{N}_0$-dependence which can be eliminated by the Empirical Interpolation Method [5, 18], we note that the dependence is linear and it still produces an approximation much faster than the original FDM scheme. From complexity analysis, this is possible because the coefficient matrix for the case with two-dimensional physical domain in Algorithm 1 is an $\mathcal{N}_0\times\mathcal{N}_0$ banded matrix with a band width $2N_x-1$. The fact that $\mathcal{N}_0=(N_x-1)(N_y+1)$ is often very large and N is typically very small and in particular $N<N_x$ are an indicator that our RB algorithm will be much faster than the iterative truth solver. This is indeed corroborated in the next section where we present numerical results.

4 Numerical examples

In this section, we show numerical results in both one- and two-dimensional spaces to demonstrate the performance of the proposed RBM algorithm. The common parameter space $\mathcal{D}\ni(D,V)$ is taken to be $\mathcal{D}=[0.08^2,0.4^2]\times[0,5]$, which is discretized by a so-called training set

$$\Xi=\{D|\sqrt{D}\in(0.08:0.02:0.4)\}\times\{(0:0.25:5)\}.$$

We also define a testing set

$$\Xi_{\text{test}}=\{D|\sqrt{D}\in(0.085:0.01:0.395)\}\times\{(0.4:0.5:4.4)\},$$

which in particular does not intersect with the training set. Here, the notation $a:h:b$ denotes an equidistant discretization of the interval $[a,b]$ by elements of size h. In addition, we let $E(N)$ represent the maximum relative error over all μ in Ξ_{test} of the reduced basis solution using N basis functions in comparison to the high-fidelity truth approximation

$$E(N)=\max_{\mu\in\Xi_{\text{test}}}\{\|\Phi(\mu)-\widehat{\Phi}(\mu)\|_\infty/\|\Phi\|_{L^\infty(\Xi_{\text{test}},L^\infty(\Omega))}\}, \tag{4.1}$$

where

$$\|\Phi\|_{L^\infty(\Xi_{\text{test}},L^\infty(\Omega))}=\max_{\mu\in\Xi_{\text{test}}}\|\Phi(\mu)\|_\infty.$$

Lastly, we let

$$\Delta_{\text{RB}}^{\max}(N)=\max_{\mu\in\Xi}\Delta_N(\mu),$$

represent the maximum error bound over the discretized set Ξ when N parameters are selected.

4.1 One dimensional space

We consider the PB equation (3.2) with source $g(x,y)=0$. The problem reduces to one dimension thanks to the homogeneity in the y direction. The high-fidelity truth approximation Φ is obtained with a central finite difference scheme in Algorithm 1. The physical domain $[-1,1]$ is divided into N_x cells by $\mathcal{N}=N_x+1$ grid points.

Fig. 1(a) displays the relative errors of the RB solution when different partition numbers $N_x=1000,2000,4000$ and 8000 are used for the high-fidelity truth approximation. One clearly observes exponential convergence of the error with respect to the number of reduced bases. For this one-dimensional problem, using $N=12$ basis functions is enough for the error $E(N)$ to reach $\sim 10^{-6}$ which is of the same magnitude as the high-fidelity truth approximation error. Fig. 1(b) shows the sample solutions $\Phi(x;\mu=(D,2))$, i.e., the potential distributions at different D values with $V=2$ and $N_x=10,000$.

The nonlinear PBE has a boundary layer near each boundary where the voltage is applied. The width of these layers are about $\mathcal{O}(\sqrt{D})$. In addition, since V dictates the Dirichlet boundary, it is clear that the smaller D is and the larger V is, the stronger the boundary-layer is. This is a manifestation of the nonlinearity of the PB equation. It provides an intuitive account of why the parameter locations for the chosen RB snapshots, shown in Fig. 1(d), cluster around the upper-left corner of the parameter domain with smaller D and larger V values. More basis are needed to resolve the boundary layer to a high accuracy in the regime of smaller D and larger V. In addition, most of the selected parameters are on the boundaries, i.e., when $V=0$ or 5 and $\sqrt{D}=0.08$ or 0.4, the latter denoted by the left ($D=0.0064$) and the right ($D=0.16$) vertical lines.

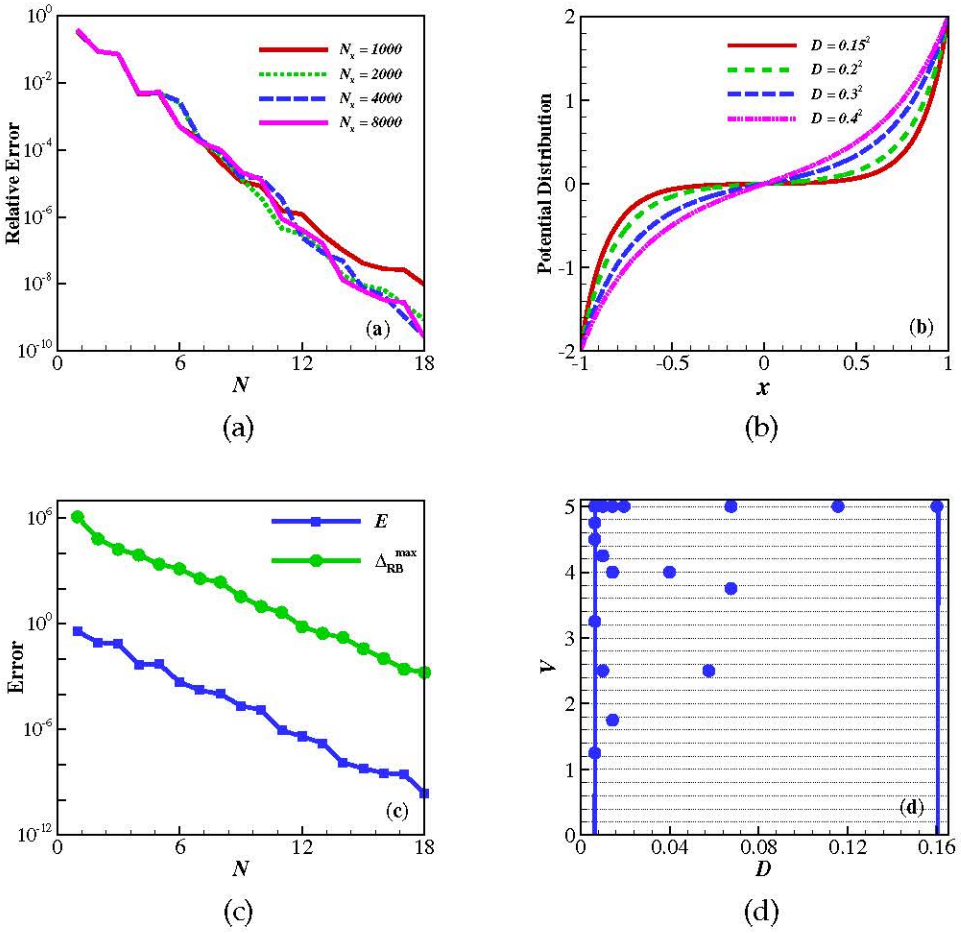

Figure 1: (a) The maximum relative errors of RB approximations $E(N)$ versus N. (b) Potential distributions at representative D values with $V=2$. (c) Maximum error estimators of RB approximation $\Delta_{\mathrm{RB}}^{\max}$ versus N. (d) The location of the selected parameters where the reduced bases are computed.

Now we fix $N_x=10{,}000$ and study the effectivity of the RB model. We show the comparison of $\Delta_{RB}^{\max}(N)$ and the RB relative error $E(N)$ in Fig. 1(c) and the selected parameters' locations in Fig. 1(d). It is noted that the error estimator is decreasing with similar exponential speed as the error even though the error is calculated in a stronger norm (L^∞) than that for the residual in the error estimator.

Next, we report the result on calculating the total differential capacitance for the symmetric electrolyte. The numerical surface charge density σ is calculated by,

$$\sigma = D\partial_x\Phi(x=-1) = D\frac{4\Phi(x_2)-3\Phi(x_1)-\Phi(x_3)}{2h} \tag{4.2}$$

upon which the differential capacitance is obtained. We take $\sqrt{D}=0.08:0.005:0.4$, $V=0:0.02:2$ and $N=16$ to calculate a surrogate differential capacitance. Fig. 2(a) shows

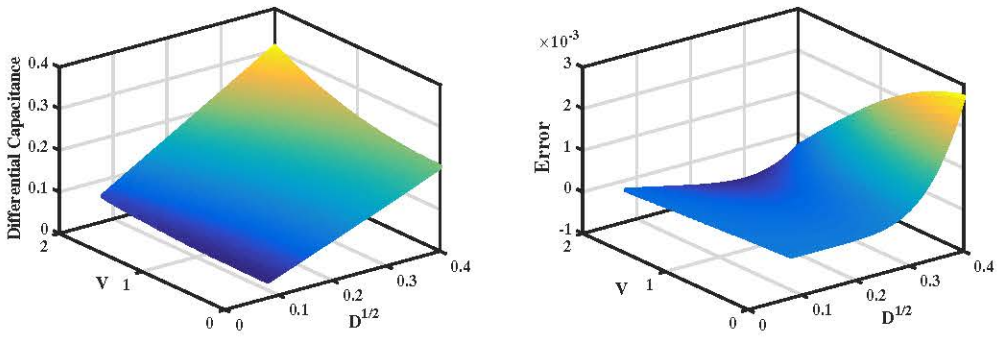

(a) (b)

Figure 2: (a) Differential capacitance C evaluated by RBM as a function of the voltage V and $\sqrt{D}$. (b) The error of the differential capacitance as function of V, $\sqrt{D}$.

the capacitance, with Φ evaluated by RBM as a function of the boundary voltage V and $\sqrt{D}$, while Fig. 2(b) shows the error surface. Here Error $=C^{acc}-C^{RBM}$, C^{acc} is calculated through expression (3.8) and C^{RBM} represent differential capacitance calculated by RBM through expression (4.2). It can be observed that the RBM is very accurate even with a small number of bases ($N=16$).

4.2 Two dimensional space

In this section, we solve a two dimensional PB equation (3.2) with the fixed charge $g(x,y)=\exp[-50(x^2+y^2)]$. The total number of nodes for the central-difference scheme in Algorithm 1 is $\mathcal{N}=(N_x+1)(N_y+1)$ and the number of unknown nodes is $\mathcal{N}_0=(N_x-1)(N_y+1)$. The boundary conditions on $y=\pm 1$ are approximated by the central difference scheme.

We first show representative RB approximations $\widehat{\Phi}$ when $D=0.04, N_x=N_y=200$ in Fig. 3. It can be observed that when the applied voltage is smaller, the variation of the potential distribution Φ is stronger.

Using the same parameter subsets as those in the previous section, we show the RB relative error $E(N)$ in Fig. 4(a) and we again observe the convergence for all partition numbers N_x, N_y with $N_x=N_y=200,400,800$. We see that, for the RBM solution to approximate the FDM sufficiently closely, a basis number N larger than the one-dimensional case is necessary. In order to show that when $N\approx 20$ we are at the FDM accuracy level, we verify our FDM accuracy in Fig. 4(b). Indeed, we set $N_x=200,400,800$ and 1,600 with $V=0.1, D=0.04$ and take the solutions with $N_x=1,600$ to be the reference and define

$$E_x(i)=||\Phi_{N_x}(i,\cdot)-\Phi_{1600}(i,\cdot)||_\infty, \quad i=1,2,\cdots,N_x+1.$$

E_x can be viewed as the absolute error at each discrete node in x-direction and the infinite norm is for the y-direction. The distribution of E_x is shown in Fig. 4(b) and clearly we

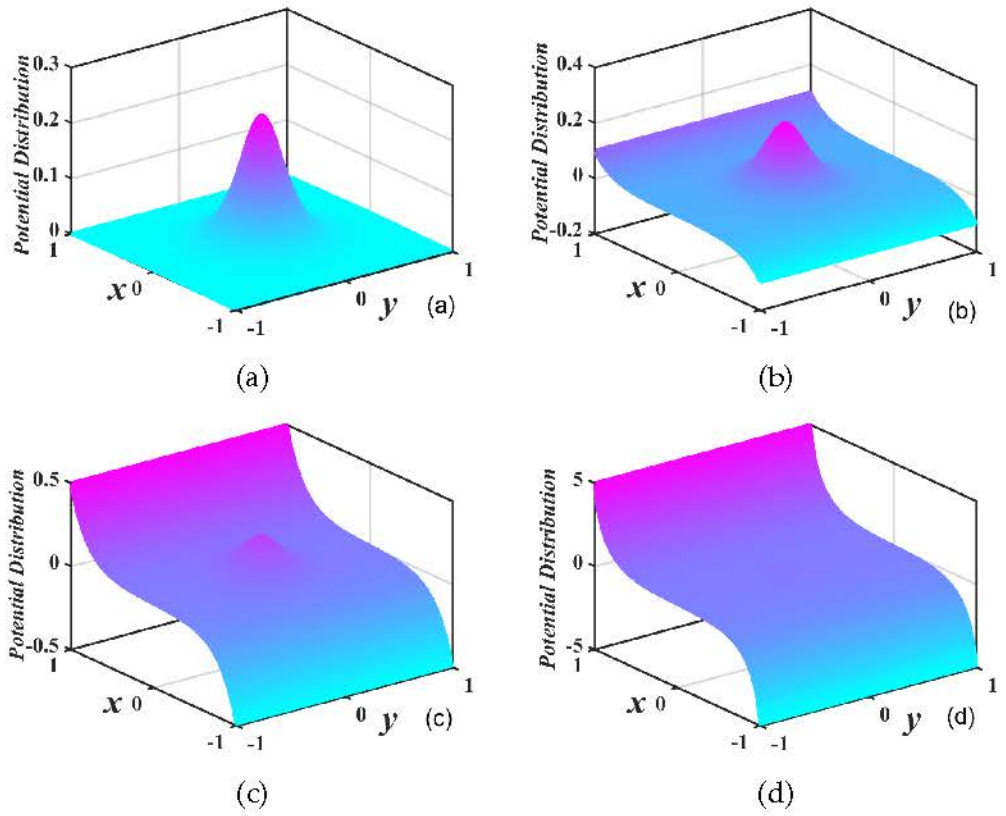

Figure 3: Potential distributions for different V by the RBM. (a) $V=0$ (b) $V=0.1$ (c) $V=0.5$ (d) $V=5$.

only need about 20 parameters to reach the high-fidelity relative error $\sim 10^{-6}$ which is the accuracy level of the FDM solution. The comparison between $E(N)$ and $\Delta_{RB}^{\max}$ when $N_x = N_y = 200$, $N = 20$ is shown in Fig. 4(c). Parameter locations for the RB snapshots are shown in Fig. 4(d) when $N_x = N_y = 200, N = 20$ and we also find that small voltages are often selected, which is consistent with the conclusions in Fig. 3. Specifically, most of selected parameters sit on the boundaries of the parameter domain and the left vertical line in Fig. 4(d) refers to $D = 0.0064$ and the right one refers to $D = 0.16$.

Next, we report the speedup attributed to the application of the RBM. The final online time consumption comparison is shown in Table 1. Obviously the online time of RB approximation is smaller than Algorithm 1. This is mainly due to the coefficient matrix structure of the two dimensional case. It is not a tridiagonal matrix as in the one dimensional case and order reduction is significant for such matrix with a wide band width. The actual speedup will also depend on a practitioner's implementation of the algorithm and the adopted computing environment. We note that these tests were performed by Matlab 2016b on a 64-bit laptop with Windows 10 operating system whose processor version is Intel(R) Core(TM) i7-6500U CPU @2.50GHz.

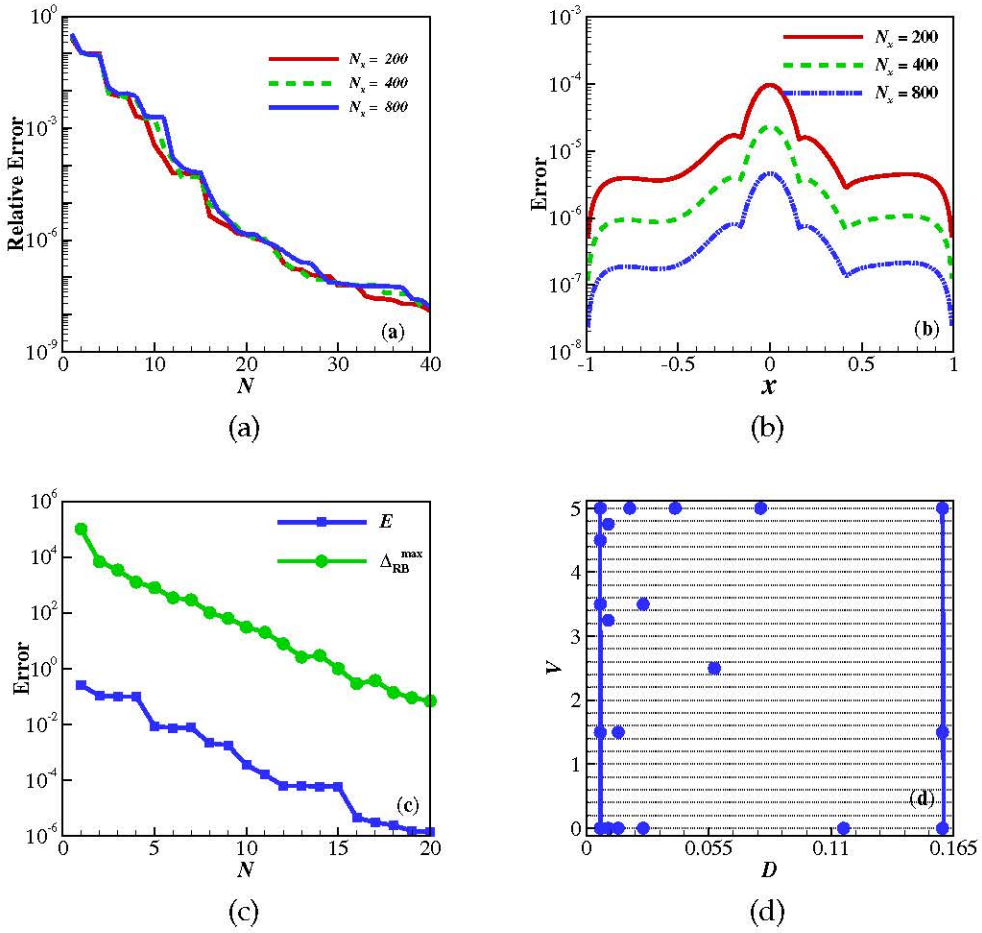

Figure 4: (a) Convergence of RB approximation of different partition numbers at different basis numbers N. (b) The error accuracy E_x of FDM in x-direction at different partition numbers N_x with $V=0.1$, $D=0.04$. (c) Maximum error estimators $\Delta_{\mathrm{RB}}^{\max}$ at different basis numbers N. (d) Selected parameters' location.

Finally, as in the one-dimensional case, we report the effectivity of using RBM to calculate the quantity of interest, namely the differential capacitance. Toward that end, we take $N_x = N_y = 400, D = 0.08:0.005:0.4$, $V = 0.04:0.02:2$ and $N = 20$. These results

Table 1: Online computational times at different partition numbers N_x, N_y when $V=3.57$, $D=0.25^2$, $N=20$.

N_x, N_y	RBM $\widehat{\Phi}$	FDM Φ
100	0.0231827	0.2228043
200	0.0960147	1.1668299
400	0.4744200	5.3805034
800	2.0143542	27.2314357

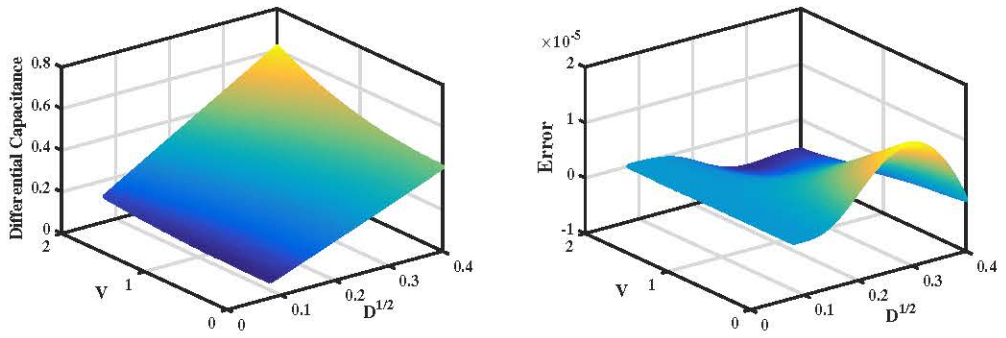

Figure 5: (a) Differential capacitance C at different voltages V and $\sqrt{D}$ by RBM. (b) Corresponding error at different voltages V and $\sqrt{D}$.

are showed in Fig. 5. In particular, the error as shown in Fig. 5(b) is defined in the same fashion as the one dimensional case. In fact, calculating these differential capacitance through the RBM is 29 or more times faster than using FDM. This demonstrates that the RBM approximation is efficient in calculating the parametrized physical quantities such as the differential capacitance of the electrochemical system.

5 Conclusions

This paper adapts the RB algorithm to solve the parametrized nonlinear PB equation in both one and two dimensional physical spaces with a two dimensional parameter space. Though PB equation is non-affine and has exponential nonlinearity, our algorithm shows good accuracy and the selected parameters' distribution accurately reflects the nonlinearity of the PB equation. In future work, we consider further enhancement to the algorithm including application of EIM achieving total $\mathcal{N}$-independence of the online solver and a novel approach that achieves the same efficiency without EIM.

Acknowledgements

L. Ji and Z. Xu acknowledge the support from grants NSFC 11571236 and 21773165 and HPC center of Shanghai Jiao Tong University. Y. Chen was partially supported by the United States National Science Foundation grant DMS-1719698. The authors are thankful to the anonymous referees whose suggestions greatly improved the presentation of this paper.

References

[1] B. O. ALMROTH, P. STERN AND F. A. BROGAN, *Automatic choice of global shape functions in structural analysis,* AIAA J., 16(5) (1978), pp. 525–528.

[2] N. A. BAKER, *Poisson–Boltzmann methods for biomolecular electrostatics,* Method Enzymol, 383 (2004), pp. 94–118.

[3] N. A. BAKER, *Improving implicit solvent simulations: A Poisson-centric view,* Curr. Opin. Struct. Biol., 15 (2005), pp. 137–143.

[4] N. A. BAKER, M. J. HOLST AND F. WANG, *Adaptive multilevel finite element solution of the Poisson–Boltzmann equation II. refinement at solvent-accessible surfaces in biomolecular systems,* J. Comput. Chem., 21(15) (2000), pp. 1343–1352.

[5] M. BARRAULT, Y. MADAY, N. C. NGUYEN AND A. T. PATERA, *An empirical interpolation method: Application to efficient reduced-basis discretization of partial differential equations,* C. R. Math., 339(9) (2004), pp. 667–672.

[6] A. H. BOSCHITSCH AND M. O. FENLEY, *Hybrid boundary element and finite difference method for solving the nonlinear Poisson–Boltzmann equation,* J. Comput. Chem., 25(7) (2004), pp. 935–955.

[7] D. L. CHAPMAN, *A contribution to the theory of electrocapillarity,* Phil. Mag., 25 (1913), pp. 475–481.

[8] L. CHEN, M. J. HOLST AND J. XU, *The finite element approximation of the nonlinear Poisson–Boltzmann equation,* SIAM J. Numer. Anal., 45(6) (2007), pp. 2298–2320.

[9] Y. CHEN, J. S. HESTHAVEN, Y. MADAY AND J. RODRÍGUEZ, *Improved successive constraint method based a posteriori error estimate for reduced basis approximation of 2D Maxwell's problem,* M2AN, 43 (2009), pp. 1099–1116.

[10] Y. CHEN, J. S. HESTHAVEN, Y. MADAY AND J. RODRIGUEZ, *Certified reduced basis methods and output bounds for the harmonic Maxwell's equations,* SIAM J. Sci. Comput., 32(2) (2010), pp. 970–996.

[11] Y. CHEN, J. S. HESTHAVEN, Y. MADAY, J. RODRIGUEZ AND X. ZHU, *Certified reduced basis method for electromagnetic scattering and radar cross section estimation,* Comput. Methods Appl. Mech. Eng., 233-236 (2012), pp. 92–108.

[12] B. E. CONWAY, Electrochemical Supercapacitors: Scientific Fundamentals and Technological Applications, Kluwer Academic/Plenum Publishers, New York, 1999.

[13] M. E. DAVIS AND J. A. MCCAMMON, *Electrostatics in biomolecular structure and dynamics,* Chem. Rev., 90(3) (1990), pp. 509–521.

[14] S. DEPARIS AND G. ROZZA, *Reduced basis method for multi-parameter-dependent steady Navier–Stokes equations: applications to natural convection in a cavity,* J. Comput. Phys., 228(12) (2009), pp. 4359–4378.

[15] F. FOGOLARI, A. BRIGO AND H. MOLINARI, *The Poisson–Boltzmann equation for biomolecular electrostatics: A tool for structural biology,* J. Mol. Biol., 15 (2002), pp. 377–392.

[16] R. H. FRENCH, V. A. PARSEGIAN, R. PODGORNIK, R. F. RAJTER, A. JAGOTA, J. LUO, D. ASTHAGIRI, M. K. CHAUDHURY, Y.-M. CHIANG, S. GRANICK, S. KALININ, M. KARDAR, R. KJELLANDER, D. C. LANGRETH, J. LEWIS, S. LUSTIG, D. WESOLOWSKI, J. S. WETTLAUFER, W.-Y. CHING, M. FINNIS, F. HOULIHAN, O. A. VON LILIENFELD, C. J. VAN OSS AND T. ZEMB, *Long range interactions in nanoscale science,* Rev. Mod. Phys., 82(2) (2010), pp. 1887–1944.

[17] G. GOUY, *Constitution of the electric charge at the surface of an electrolyte,* J. Phys., 9 (1910), pp. 457–468.

[18] M. A. GREPL, Y. MADAY, N. NGUYEN AND A. T. PATERA, *Efficient reduced-basis treatment of nonaffine and nonlinear partial differential equations,* ESAIM Math. Model. Numer. Anal., 41(3) (2007), pp. 575–605.
[19] B. HAASDONK, Chapter 2: Reduced Basis Methods for Parametrized PDEs–A Tutorial Introduction for Stationary and Instationary Problems, pages 65–136.
[20] B. HAASDONK, M. DIHLMANN AND M. OHLBERGER, *A training set and multiple bases generation approach for parameterized model reduction based on adaptive grids in parameter space,* Math. Comput. Model. Dyn. Sys., 17(4) (2011), pp. 423–442.
[21] B. HAASDONK AND M. OHLBERGER, *Reduced basis method for finite volume approximations of parametrized linear evolution equations,* M2AN Math. Model. Numer. Anal., 42(2) (2008), pp. 277–302.
[22] J. S. HESTHAVEN, G. ROZZA AND B. STAMM, *Certified reduced basis methods for parametrized partial differential equations,* SpringerBriefs in Mathematics, Springer, Cham; BCAM Basque Center for Applied Mathematics, Bilbao, 2016, BCAM SpringerBriefs.
[23] J. S. HESTHAVEN, B. STAMM AND S. ZHANG, *Efficient greedy algorithms for high-dimensional parameter spaces with applications to empirical interpolation and reduced basis methods?,* ESAIM: Math. Model. Numer. Anal., 48(1) (2014), pp. 259–283.
[24] D. B. P. HUYNH, D. J. KNEZEVIC, Y. CHEN, J. S. HESTHAVEN AND A. T. PATERA, *A natural-norm successive constraint method for inf-sup lower bounds,* CMAME, 199 (2010), pp. 1963–1975.
[25] D. B. P. HUYNH, G. ROZZA, S. SEN AND A. T. PATERA, *A successive constraint linear optimization method for lower bounds of parametric coercivity and inf-sup stability constants,* C. R. Acad. Sci. Paris, Série I., 345 (2007), pp. 473–478.
[26] J. JIANG, Y. CHEN AND A. NARAYAN, *Offline-enhanced reduced basis method through adaptive construction of the surrogate training set,* J. Sci. Comput., 73(2) (2017), pp. 853–875.
[27] P. JORDAN, R. BACQUET, J. MCCAMMON AND P. TRAN, *How electrolyte shielding influences the electrical potential in transmembrane ion channels,* Biophys. J., 55(6) (1989), pp. 1041–1052.
[28] C. KWEYU, L. FENG, M. STEIN AND P. BENNER, *Fast solution of the linearized Poisson–Boltzmann equation with nonaffine parametrized boundary conditions using the reduced basis method,* preprint arXiv:1705.08349, 2017.
[29] C. KWEYU, M. HESS, L. FENG, M. STEIN AND P. BENNER, *Reduced basis method for Poisson–Boltzmann equation,* in Proceedings of VII European Congress on Computational Methods in App. Sci. Eng., (2016), pp. 4187–4195.
[30] Y. LEVIN, *Electrostatic corrections: from plasma to biology,* Rep. Prog. Phys., 65 (2002), pp. 1577–1632.
[31] D. LEVITT, *Strong electrolyte continuum theory solution for equilibrium profiles, diffusion limitation and conductance in charged ion channels,* Biophys. J., 48(1) (1985), pp. 19–31.
[32] P. LIU, X. JI AND Z. XU, *Modified Poisson–Nernst–Planck model with accurate Coulomb correlation in variable media,* SIAM J. Appl. Math., 78 (2018), pp. 226–245.
[33] B. LU, D. ZHANG AND J. A. MCCAMMON, *Computation of electrostatic forces between solvated molecules determined by the Poisson–Boltzmann equation using a boundary element method,* J. Chem. Phys., 122(21) (2005), 214102.
[34] B. LU, Y. ZHOU, M. J. HOLST AND J. A. MCCAMMON, *Recent progress in numerical methods for the Poisson–Boltzmann equation in biophysical applications,* Commun. Comput. Phys., 3 (2008), pp. 973–1009.
[35] A. K. NOOR AND J. M. PETERS, *Reduced basis technique for nonlinear analysis of structures,* AIAA J., 18(4) (1980), pp. 455–462.
[36] A. QUARTERONI, A. MANZONI AND F. NEGRI, Reduced Basis Methods for Partial Differ-

ential Equations: An Introduction, Volume 92, Springer, 2015.

[37] G. ROZZA, D. B. P. HUYNH AND A. T. PATERA, *Reduced basis approximation and a posteriori error estimation for affinely parametrized elliptic coercive partial differential equations,* Arch. Comput. Methods Eng., 15(3) (2008), pp. 229–275.

[38] S. SEN, *Reduced-basis approximation and a posteriori error estimation for many-parameter heat conduction problems,* Numerical Heat Transfer, Part B: Fundamentals, 54(5) (2008), pp. 369–389.

[39] A. I. SHESTAKOV, J. L. MILOVICH AND A. NOY, *Solution of the nonlinear Poisson–Boltzmann equation using pseudo-transient continuation and the finite element method,* J. Colloid Interf. Sci., 247(1) (2002), pp. 62–79.

[40] K. URBAN, S. VOLKWEIN AND O. ZEEB, *Greedy sampling using nonlinear optimization,* in Reduced Order Methods for Modeling and Computational Reduction, pages 137–157, Springer, 2014.

[41] K. VEROY, C. PRUD'HOMME AND A. T. PATERA, *Reduced-basis approximation of the viscous Burgers equation: rigorous a posteriori error bounds,* C. R. Math., 337(9) (2003), pp. 619–624.

[42] D. A. WALKER, B. KOWALCZYK, M. O. DE LA CRUZ AND B. A. GRZYBOWSKI, *Electrostatics at the nanoscale,* Nanoscale, 3 (2011), pp. 1316–1344.

[43] P. WEETMAN, S. GOLDMAN AND C. GRAY, *Use of the Poisson–Boltzmann equation to estimate the electrostatic free energy barrier for dielectric models of biological ion channels,* J. Phys. Chem. B, 101(31) (1997), pp. 6073–6078.

[44] D. S. WEILE, E. MICHIELSSEN AND K. GALLIVAN, *Reduced-order modeling of multiscreen frequency-selective surfaces using Krylov-based rational interpolation,* IEEE Trans. Antennas Propagat., 49 (2001), pp. 801–813.